Journal of Industrial and Management Optimization

JIMO, 22(2): 1168–1193.
DOI: 10.3934/jimo.2026043
Received: 16 September 2025
Revised: 20 December 2025
Accepted: 22 January 2026
Published: 30 January 2026

https://www.aimspress.com/journal/jimo

Research article

Joint optimization of selective maintenance decision-making and maintenance personnel allocation under limited resources

Yang Jiao[1], Qiu-Xiang Tao[2,*], Hui Liu[2], Qi-Rui Peng[1] and Zhi-Cheng Zhou[1]

[1] College of Economics and Management, Nanchang Hangkong University, Nanchang 330063, China
[2] School of Information Engineering, Nanchang Hangkong University, Nanchang 330063, China

* **Correspondence:** Email: czp8266588733@163.com.

Abstract: Integrating selective maintenance strategies with personnel allocation for equipment groups is essential to meet combat missions' demands and significantly boost overall combat effectiveness. Accordingly, this study aims to maximize the probability of mission completion for equipment groups by developing a joint optimization model under constrained resource conditions. An environmental coefficient is incorporated to represent the dynamic impact of varying combat environments on the degradation states of individual units. Using a nonhomogeneous Markov model, this study calculates the state transition probabilities of units throughout the mission to derive the mission completion probabilities for both the equipment group and the overall combat cycle. To solve this model, an adaptive quantum immune algorithm is applied to the case study. These findings demonstrate that the proposed model and algorithm enhance maintenance decision-making quality and clarify optimization patterns regarding resource efficiency and dynamic personnel allocation. Thus they offer both a theoretical foundation and practical guidance for battlefield maintenance support.

Keywords: selective maintenance; allocation of maintenance personnel; joint optimization; adaptive quantum immune algorithm
Mathematics Subject Classification: 90B25, 90B35

1. Introduction

Modern informatized warfare relies heavily on combat forces composed of equipment groups integrating diverse subunits. To ensure the optimal operational performance of these equipment groups,

it is essential to implement maintenance strategies that are appropriately aligned with the requirements of combat missions. However, battlefield constraints, especially limited maintenance resources, often preclude the comprehensive repair of all degraded equipment. Consequently, there is a critical need to develop an integrated approach that determines the optimal maintenance plan. This approach must synthesize the real-time condition of the equipment, the mission's demands, and resource constraints to simultaneously optimize the selection of maintenance targets and measures, and the allocation of personnel. Addressing this challenge constitutes a critical and urgent priority within the current field of equipment support [1].

Selective maintenance decision-making is widely recognized as an effective strategy for optimizing maintenance activities under conditions of limited resources and has attracted considerable scholarly attention. Previous research has primarily focused on multiobjective optimization [2–5], the allocation of multiple maintenance personnel [6–9], and scenarios involving multiple tasks [10–13]. Over the past five years, Wei-Ning Ma et al. has investigated the independent optimization challenges related to selective maintenance decisions and task allocation, aiming to maximize the probability of task completion. They concluded that incorporating combat task allocation improves outcomes [14]. Amjadian et al. extended the fleet selective maintenance problem (FSMP) by including asynchronous maintenance intervals and resource constraints, linking the selective maintenance problem (SMP) to the resource-constrained project scheduling problem (RCPSP). Their numerical experiments highlighted key trade-offs to guide optimal system performance decisions [15]. Similarly, You-Peng Zhang et al. examined the impact of the number of maintenance personnel on the system's maintenance costs and downtime, with the objective of enhancing the system's reliability and availability while minimizing maintenance expenses. Their findings suggested that a maintenance team comprising six personnel is optimal [16]. Chaabane's study demonstrated that mixed-skill maintenance teams are more cost-effective than single-skill teams in battlefield environments [17]. Furthermore, Moghaddam et al. explored selective maintenance decision methodologies within wartime maintenance contexts, emphasizing maximization of the systems' reliability [18]. O'Neil et al. proposed a model for jointly optimizing selective maintenance scheduling and task abortion decisions in a three-module critical system. By maintaining components during halftime breaks to minimize performance degradation for subsequent tasks, the model enhances the probability of task success and system survivability compared with strategies without task abortion [19].

Despite these contributions, significant gaps remain when applying the existing frameworks to complex battlefield environments, particularly in the following aspects.

(1) Separately optimizing maintenance measures and personnel allocation risks strategic failure due to resource overextension in complex battlespaces. This necessitates an integrated framework that jointly considers maintenance actions, personnel skills, and resource constraints.

(2) Existing models fail to quantify the resource efficiency boundaries of different skill combinations or capture the dynamic personnel demands caused by resource fluctuations in multitask scenarios. This gap highlights the urgent need for adaptive mechanisms to reconfigure personnel teams under resource constraints, ensuring continuous support across sequential missions.

In response to these challenges, this study presents a nonhomogeneous Markov model to dynamically capture the effects of battlefield environment changes and equipment fatigue on unit degradation. It develops an integrated triune joint optimization model combining maintenance selection, personnel skill adaptation, and dynamic resource coordination to maximize the probability of task completion under mission reliability and resource constraints. The adaptive quantum immune

algorithm (AQIA) integrates a scheduling feedback mechanism with quadrant decision evolution, maintaining the population's feasibility in complex coupled optimization problems. This model elucidates resource efficiency patterns and dynamic personnel allocation, offering dynamic decision support for battlefield equipment maintenance and support.

2. Overview of the decision-making framework

2.1. Technical approach and assumptions

The technical methodology underpinning the selective maintenance decision-making model for equipment groups developed in this study is described in detail below.

Step 1: Define the degradation patterns of multistate units along with the corresponding maintenance effects. Subsequently, the rules for selecting appropriate maintenance measures are formulated. Furthermore, a task completion evaluation framework is established, a resource scheduling mechanism is developed, and a dynamic evaluation system for personnel's skill levels is constructed.

Step 2: Formulate a joint optimization objective model that maximizes the overall completion probability of multiple tasks, while adhering to dual constraints regarding total cost and time windows.

Step 3: Develop an AQIA to implement quantum information feedback by encoding maintenance measures into the quantum states, coupled with a coordinated resource scheduling mechanism.

Step 4: Solve the model using the AQIA implemented in MATLAB. This solution yields the overall probability of completing multiple tasks under resource constraints and identifies the optimal selective maintenance scheme for the equipment group. The scheme specifies which units require maintenance, the maintenance measures assigned to each unit, and the scheduling of maintenance personnel. Furthermore, the analysis investigates the effects of personnel structure thresholds and resource efficiency intervals on the optimization objectives.

The fundamental assumptions underlying the model are as follows:

(1) The equipment ensemble experiences degradation exclusively throughout the operational mission period, with no degradation occurring during maintenance intervals.

(2) The length of combat missions is subject to dynamic variation; upon completion of maintenance, the equipment ensemble promptly initiates the subsequent combat mission.

(3) There is no predetermined sequence for the maintenance of individual subunits within the equipment ensemble; maintenance activities may be conducted simultaneously.

(4) The equivalent duration of maintenance and the associated costs for a single repair of a subunit encompass all constituent components and are not further disaggregated.

2.2. The fundamental operational level of the combat unit

2.2.1. Definition of multistate systems

The equipment group is defined as consisting of multiple combat units that are not completely homogeneous. Each combat unit is represented as a multistate system with i distinct states, where state S_1 indicates a total failure condition, state S_i signifies a fully operational condition, and the intermediate $i-2$ states correspond to partial operational conditions [20]. The system under

investigation in this study is categorized into five distinct states, with the performance loss associated with each state presented in Table 1 below.

Table 1. Definition of the ground state.

Equipment status	Status name	Core function description	Performance loss threshold
S1	Entirely ineffective	Loss of essential functionality	$80\% < L_1 \leq 100\%$
S2	Significant deterioration	Core function is significantly impaired	$60\% \leq L_2 < 80\%$
S3	Moderate deterioration	Core function is partially impaired	$40\% \leq L_3 < 60\%$
S4	Slight deterioration	Core function is essentially standard	$20\% \leq L_4 < 40\%$
S5	Functioning properly	Core function remains intact	$L_5 < 20\%$

The dynamics of the state transitions for the entire system can be characterized by the state transition intensity matrix Λ_0, defined as follows:

$$\Lambda_0 = \begin{bmatrix} 0 & 0 & 0 & 0 & 0 \\ \lambda_{21} & -\lambda_{21} & 0 & 0 & 0 \\ \lambda_{31} & \lambda_{32} & -(\lambda_{31}+\lambda_{32}) & 0 & 0 \\ \lambda_{41} & \lambda_{42} & \lambda_{43} & -(\lambda_{41}+\lambda_{42}+\lambda_{43}) & 0 \\ \lambda_{51} & \lambda_{52} & \lambda_{53} & \lambda_{54} & -(\lambda_{51}+\lambda_{52}+\lambda_{53}+\lambda_{54}) \end{bmatrix}.$$

In this formula, the element λ_{ij} located at the ith row and jth column represents the transition rate from state S_i to a lower energy state S_j. Conventional homogeneous Markov models, characterized by constant transition rates, are inadequate for capturing the effects of varying task environments. Therefore, a nonhomogeneous Markov model is proposed to accurately quantify the degradation of each unit's state during the task's performance. The associated mathematical formulation is provided below:

$$\Lambda_m(t) = \alpha_m \cdot \Lambda_0 \cdot (1 + \beta t). \tag{2.1}$$

In this formula, the environmental coefficient α_m quantifies the severity of the conditions under which the combat mission is conducted, whereas the coefficient β represents the degree of performance degradation experienced by each unit through accumulated fatigue. The dynamic degradation behavior of the unit throughout the mission is modeled using the Kolmogorov differential equation, which is expressed as follows:

$$\begin{gathered} \frac{dP_u(t)}{dt} = P_u(t) \cdot \Lambda_m(t), \\ P_u(t) = [P_u(S_1,t), P_u(S_2,t), P_u(S_3,t), P_u(S_4,t), P_u(S_5,t)], \\ \sum_{s=1}^{5} P_u(S_s,t) = 1. \end{gathered} \tag{2.2}$$

In the formula above, $P_u(t)$ represents the probability distribution of the states of unit u at time t. The state transition process described in this article is illustrated in Figure 1.

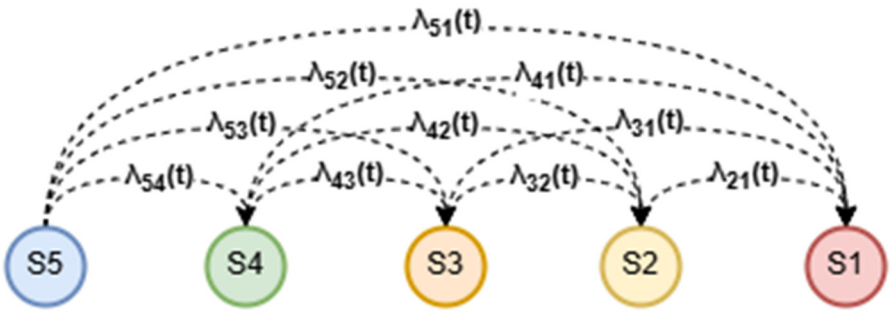

Figure 1. Example of state transition.

2.2.2. Modeling the effectiveness of maintenance activities

Maintenance activities are performed on equipment at predetermined task intervals with the objective of restoring the equipment to an improved operational state. Based on performance degradation, a set of maintenance measures, denoted $v \in \{0,1,2,3,4\}$, is defined, with its elements corresponding, respectively, to no maintenance, three forms of imperfect maintenance, and perfect maintenance. The corresponding maintenance effect matrix, A_v, is provided below:

$$A_v = \begin{bmatrix} a_{1,1}^v & a_{1,2}^v & a_{1,3}^v & a_{1,4}^v & a_{1,5}^v \\ 0 & a_{2,2}^v & a_{2,3}^v & a_{2,4}^v & a_{2,5}^v \\ 0 & 0 & a_{3,3}^v & a_{3,4}^v & a_{3,5}^v \\ 0 & 0 & 0 & a_{4,4}^v & a_{4,5}^v \\ 0 & 0 & 0 & 0 & 1 \end{bmatrix}. \tag{2.3}$$

In this context, element $a_{i,j}^v$ denotes the probability that a unit initially in State i transitions to State j following the implementation of maintenance measure v. Each element within a row satisfies the condition $\sum_{j=i}^{5} a_{i,j}^v = 1$. Combining the hierarchical definition of performance degradation, a repair's effectiveness is directly linked to the degradation threshold levels. After a complete repair, the unit returns to full functionality. The effectiveness of partial repairs varies dynamically with the amount of repair resources invested—the more resources allocated, the greater the likelihood the unit will achieve a better state post-repair.

Consequently, if the initial state probability distribution of the unit at the commencement of the task interval is denoted by $P_u(t)$, then the state probability distribution following the implementation of the maintenance actions can be expressed as follows:

$$P_{unew} = P_u(t) \cdot A_v. \tag{2.4}$$

2.3. Decision-making hierarchy in the maintenance strategy formulation

2.3.1. Modeling criteria for the alignment of maintenance strategies

Each unit has a unique initial state probability and, therefore, a distinct maintenance strategy, leading to differing state probability distributions following maintenance. The maintenance decision matrix is formally defined as follows:

$$X_{muv} \in \{0,1\}, \forall m \in M,\ u \in U_m. \tag{2.5}$$

In this formula, M denotes the set of equipment groups, U_m represents the set of units contained within the equipment group m, and $X_{muv} = 1$ signifies the selection of the maintenance measure v applied to the unit u within the equipment group m. The criteria for aligning maintenance actions with their respective units are as follows:

$$s.t. \begin{cases} \sum_v X_{muv} = 1, \forall (m,u) \\ X_{mu0} = 0, if\,(m,u) \in U_{Prohibited} \end{cases}. \tag{2.6}$$

In this formula, Rule 1 stipulates that each unit may select only one type of maintenance measure. Rule 2 specifies that if a unit (m, u) is an element of the subset $U_{Prohibited}$ (critical units that require maintenance), the no maintenance option ($v = 0$) is disallowed. This condition explicitly mandates that critical units cannot remain unmaintained and must instead select one of the maintenance measures corresponding to $v = 0$ to $v = 4$.

2.3.2. An analysis of task completion rates within equipment groups

The transition matrix is updated in accordance with the selection variable related to the maintenance measures. When event $X_{muv} = 1$ occurs, the state probability distribution of an individual unit is represented by P_{unew}. The completion level of a single piece of equipment is defined by the nonfailure states S_i of the individual units that constitute the equipment group. Specifically, we require that at least K_m units within the equipment group U_m remain operational without failure. Consequently, the task completion degree function D_m for the equipment group can be formulated as follows:

$$D_m = \sum_{j=K_m}^{U_m} \binom{U_m}{j} \left(\sum_{i=2}^{5} P_{unew}(S_i)\right)^j \cdot \left(1 - \sum_{i=2}^{5} P_{unew}(S_i)\right)^{U_m - j}. \tag{2.7}$$

In this formula, $\sum_{i=2}^{5} P_{unew}(S_i)$ represents the overall probability that unit u remains functional after the repair process.

2.4. Layer for scheduling resource utilization

2.4.1. Modeling the skill levels of maintenance personnel

Considering that the proficiency levels of maintenance personnel directly affect their effectiveness, and recognizing the variability in expertise across different maintenance techniques among staff, assigning a maintenance skill level based on a single metric does not accurately reflect their true capabilities. Therefore, a maintenance technician p can be characterized by n distinct maintenance skills, which are collectively represented by a skill vector as follows:

$$s_p = [s_{p1}, \cdots, s_{pn}]\ . \tag{2.8}$$

In this formula, the variable s_{pn} represents the proficiency level of individual p in the skill category n, with s_{pn} taking values within the interval from 0 to 1. Moreover, by using the skill vector, a formula has been developed to quantify the skill levels of personnel as follows:

$$l_{pn} = \left\lfloor L_{max} \cdot \sum_{n=1}^{N} \varpi_n s_{pn} + 0.5 \right\rfloor,$$
$$\sum \omega_n = 1. \tag{2.9}$$

2.4.2. Modeling of labor hours and costs for maintenance personnel

During the execution of maintenance activities, resource constraints become evident, particularly concerning the availability of maintenance person-hours and the associated costs. It is established that the maintenance personnel possess specific benchmark person-hour equivalents (t_l) and benchmark cost equivalents (c_l) when performing maintenance tasks classified as Grade l. When the personnel undertake tasks below their designated maintenance grade, they are entitled to receive opportunity remuneration reflecting the skill premium, which concurrently incurs opportunity time. Consequently, personnel with higher skill levels require less time to complete a given task; however, this increased efficiency is accompanied by higher costs. This relationship can be formally expressed as follows:

$$t_{lnew} = t_l \cdot \left[1 - \gamma \cdot \left(l_{pn} - l_{min}\right)\right],$$
$$c_{lnew} = c_l \cdot \left[1 + \varphi \cdot \left(l_{pn} - l_{min}\right)\right]. \tag{2.10}$$

In these formulae, the variables t_l and c_l denote the benchmark resource equivalents corresponding to the minimum personnel grade required to perform maintenance activities on a specific unit. The variables l_{max} and l_{min} represent, respectively, the highest skill level of personnel and the minimum personnel grade necessary to execute the tasks associated with the current unit; $l_{pn} \geq l_{min}$ indicates the constraint that prohibits personnel of lower grades from undertaking maintenance tasks assigned to higher-grade personnel. The variables γ and φ correspond to the work hour compression coefficient and the cost increase coefficient, respectively, both of which are restricted to values within the interval from 0 to 1.

2.4.3. Modeling scheduling mechanisms incorporating degraded resource allocation and compensation strategies

Let the resource allocation matrix be denoted by Y, where Y_{usdp} represents the start time, duration, and assigned personnel for unit u. In cases where the initial resource allocation proves unsuccessful, the innovation mechanism enables resource release by dynamically reducing the maintenance levels of selected units. This method facilitates the derivation of a feasible solution that complies with resource constraints. Simultaneously, any surplus resources identified within the feasible solution are reallocated to restore maintenance levels, thereby promoting adaptive evolution and improving the overall quality of the plan. The detailed procedure and corresponding flowchart (Figure 2) are presented below.

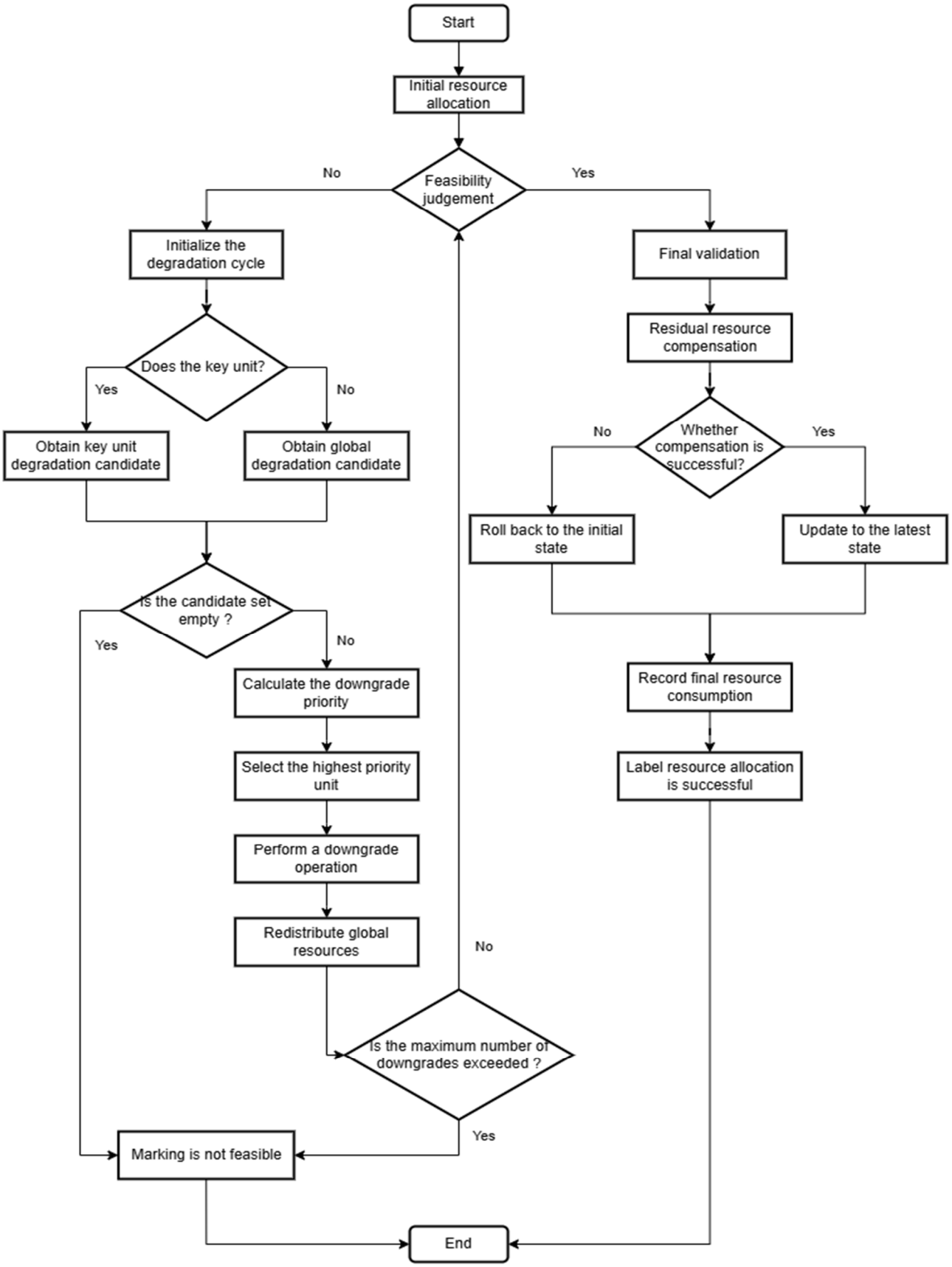

Figure 2. Flowchart depicting the allocation and compensation processes for degradable resources.

Step 1: This step involves creating a prioritized queue for critical units through initial resource allocation and assigning personnel to specific tasks. The scheduling of time windows utilizes a gap detection methodology; subject to personnel availability constraints, the earliest feasible start time is determined accordingly as follows:

$$EST(u) = min\{\, a_i \in \mathcal{A}_p | (b_i - a_i) \geq t_u\},$$
$$\mathcal{A}_p = \{[a_i, b_i] | i = 1,2,\ldots,k\}. \tag{2.11}$$

In this formula, a_i and b_i denote the start and end times of the ith available time slot, respectively; t_u denotes the time required to perform maintenance on unit u; and $\mathcal{A}_p$ represents the set of time windows. Following the initial allocation of resources, we verify whether the global resource constraints have been satisfied. If these constraints are met, we generate the feasible plan and bypass the degradation decision loop. Otherwise, we identify and report the nature of the failure and proceed to the degradation decision loop.

Step 2: The d decision process involves identifying the type of failure. When the failure occurs within a critical unit allocation, only the critical units are selected for degradation. In contrast, if the failure is noncritical or arises from resource overrun, a broader selection of degradable units is considered. Multiple categories of degradation candidate sets are automatically generated, based on the unit hierarchy within the current configuration

$$\mathcal{D}_{\text{crit}} = \{u \in U_{\text{crit}} | v_u \geq 2\},$$
$$\mathcal{D}_{\text{global}} = \{u \in U | v_u \geq 1\}. \tag{2.12}$$

In this formula, U_{crit} denotes the set of key units and v_u denotes the current maintenance level of unit u. If both the candidate degradation set and the summation are empty, the degradation decision loop terminates, and the current individual unit's resource allocation is considered to be unsuccessful. Otherwise, after recording the resource consumption, the candidate downgrade set is iterated to identify the unit with the highest priority for downgrade. The primary procedure involves calculating the reliability impact factor

$$I(u) = 1 - A_u^d. \tag{2.13}$$

In this formula, the variable A_u^d represents the probability of degradation occurring in the absence of any intervention.

The resource-saving factor is calculated as follows:

$$(u) = \frac{\Delta C_u}{C_{max}\frac{\Delta T_u}{T_{max}}}. \tag{2.14}$$

In this formula, the variables ΔC_u and ΔT_u represent the amount of resources conserved after a single stage of degradation, whereas C_{max} and T_{max} correspond to the overall constraints on resource availability.

The level of the protection factor is calculated as

$$R(u) = \begin{cases} \lambda_{\text{high}} & \text{if } u \in U_{\text{crit}} \text{ and } v_u \geq 3 \\ \lambda_{\text{mid}} & \text{if } u \in U_{\text{crit}} \text{ and } v_u = 2. \\ \lambda_{\text{low}} & \text{if } u \notin U_{\text{crit}} \end{cases} \tag{2.15}$$

In this formula, λ denotes the level of protection corresponding to various grade requirements and can be determined by experts. Considering the three factors previously mentioned, the prioritization for downgrading candidate units is established as follows:

$$P(u) = -\omega_1 \cdot I(u) + \omega_2 \cdot S(u) + \omega_3 \cdot R(u). \tag{2.16}$$

In this formula, all weights are derived from key equipment wartime maintenance data presented in this paper, using data calculation and crossvalidation. The simulated analytic hierarchy process (AHP) designs multiple candidate weight sets, selecting the combination with the highest stability. For rapid implementation, equivalent weights can be directly obtained via AHP.

Ultimately, the candidate unit with the highest priority is selected to undergo the degradation procedure, followed by a global reallocation of resources. If the current configuration proves feasible, the degradation loop exits. Otherwise, the iteration continues until the maximum cycle count is reached, at which point the resource allocation for that individual is marked as a failure.

Step 3: Conduct two comprehensive completeness assessments on the set of feasible plans. These assessments should confirm that all critical units have undergone maintenance and that units requiring maintenance have been allocated the necessary resources. Upon completion of this verification, calculate the surplus resources available. Next, all candidate units eligible for surplus resource allocation are identified. Any surplus is then allocated with priority given to upgrading noncritical units during their idle time windows. If the proposed upgrade is feasible, update the unit's status accordingly and record the final resource consumption. Should the upgrade prove unfeasible, revert the system to its original feasible state prior to the attempted upgrade. The condition governing the feasibility of surplus resource allocation is as follows:

$$\exists p \in \mathcal{P}, \exists [b_i - a_i] \in \mathcal{A}_p \text{ such that } [(b_i - a_i) \geq t_v] \wedge [C_{\text{total}} + c_v \leq C_{\max}]. \tag{2.17}$$

In this formula, the symbol $\mathcal{P}$ represents the set of qualified personnel, t_v and c_v denote the resource consumption associated with the upgraded maintenance measure v, and C_{total} indicates the total cost of the plan prior to the upgrade.

Upon the successful completion of the aforementioned procedures, the allocation of resources may be formally deemed to be successful.

3. Combined optimization objective function

On the basis of the problem descriptions of the operational unit's foundational layer (Section 2.2), the maintenance decision-making layer (Section 2.3), and the resource utilization scheduling layer (Section 2.4) as previously delineated, this study develops an integrated optimization model for selective maintenance decision-making and personnel allocation under resource constraints. The principal objective of the model is to maximize the overall mission completion rate across all equipment groups throughout the entire operational period, as illustrated in Figure 3.

$$\begin{aligned} &MaxD_{total} = \prod_{m=1}^{M} D_m \\ s.t. &\begin{cases} C_{total} = \sum_{m,u} c_{lnew} \\ T_{total} = \max\left(t_s + t_{lnew}\right) \\ C_{total} \leq C_{max}, T_{total} \leq T_{max} \end{cases} \end{aligned} . \tag{3.1}$$

The first equation shows that the individual equipment groups function independently, with the overall task completion level of the entire process being the product of the completion levels of each

equipment group (D_m). The second defines the total equivalent cost (C_{total}) associated with the maintenance process. The third equation specifies that the total duration of the maintenance process (T_{total}) corresponds to the maximum completion time observed among the units within the equipment groups. Finally, the fourth equation expresses the global finite resource constraints (C_{max}, T_{max}) imposed throughout the maintenance process.

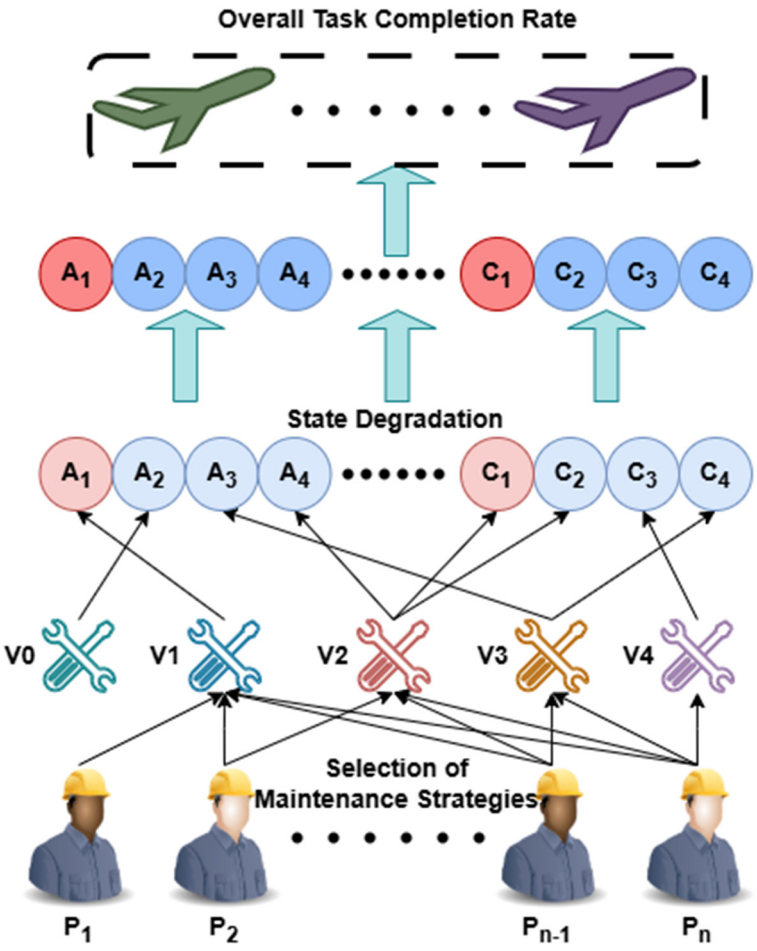

Figure 3. Relationship between maintenance strategy and the equipment group's task completion rate.

4. Problem-solving using an AQIA

To address the challenge of decoupling the optimization arising from the complex interdependence between maintenance decision-making and resource allocation, this study uses an enhanced AQIA [21–24] for optimization purposes. The work makes three primary contributions. First, it expands the solution space by encoding maintenance strategies via quantum state superposition, which allows a single individual to represent an exponentially large number of potential maintenance schemes. Second, it develops a quantum state feedback mechanism to coordinate the scheduling process, thereby achieving explicit decoupling between the decision variables and the resource constraints. Third, it formulates a four-quadrant decision model that dynamically adjusts the search direction by leveraging disparities among elite antibodies, a strategy that effectively guides the population toward the Pareto front. The primary algorithmic parameters used in this study are outlined in Table 2, and the detailed procedural methodology is described below.

Table 2. Primary algorithmic parameters.

Parameter symbol	Default value
N_{pop}	200
G_{max}	50
r	1.2
r_{elite}	0.1
r	0.2
P_c	0.55
a	0.7
t_s	0.5
t_c	0.7
P_c	0.55
P_m	0.8
θ	$\pi/25$
θ_b	$\pi/27$
η_s	0.01
η_e	0.025
η_d	0.02

Step 1: Initialize the population by encoding it through quantum state superposition.

For each antibody, initialize a quantum state matrix with elements comprising random complex numbers. Subsequently, normalize each row to ensure that the level of probability corresponding to the five maintenance measures for each maintenance unit satisfies the following normalization condition:

$$\alpha_{u,v} = r_1 + i \cdot r_2,$$
$$\|\alpha_u\|^2 = \sum_{v=0}^{4} |\alpha_{u,v}|^2 = 1. \tag{4.1}$$

Step 2: Initialize the population by using selective full collapse decoding.

For non-elite antibodies with unallocated resources, maintenance actions are selected randomly according to the probability distribution $p_{u,v} = |\alpha_{u,v}|^2$, subject to the constraint that critical unit failures cannot be assigned to the maintenance measure V_0. Upon restoration of the failed antibodies, the maintenance decision matrix X is updated, and the associated resources are reclassified as unallocated.

Step 3: Population viability assessment and maintenance.

Initially, resources are allocated to antibodies classified as unassigned through a scheduling mechanism. Subsequently, by incorporating a quantum state feedback mechanism, the physical information of the antibodies is transmitted to the quantum state, whereby the selection probabilities of the corresponding maintenance strategies within the quantum state are increased through feedback

$$\alpha^{(new)}(u, v_{\text{actual}}) = \alpha(u, v_{\text{actual}}) \cdot \text{r}. \tag{4.2}$$

In this formula, the variable r represents the reinforcement learning factor. Finally, we calculate the overall task completion rate of the current population, including elite antibodies, to determine the fitness value of each antibody.

Step 4: Immunological methodology.

Initially, the quantity of elite antibodies (N_{elite}) is determined dynamically using a nonlinear decrement method. Antibodies exhibiting the highest fitness values are selected and directly retained within the memory library. Secondly, for non-elite antibodies ($N_{pop} - N_{elite}$), we select the antibody exhibiting the lowest fitness ($N_{contrarian}$) and apply a local positional inversion to produce an enhanced antibody. Finally, the remaining non-elite antibodies ($N_{non-elitle} - N_{contrarian}$) undergo cloning according to their reproduction probabilities (p), with priority accorded to those possessing higher probabilities. This process also involves suppressing antibodies with excessively high concentrations and eliminating those with very low fitness, thereby maintaining the total population size at N_{pop}.

For each generation within the population, the quantities of elite antibodies and reverse antibodies are determined using the following calculations:

$$N_{elite} = \left\lfloor r_{elite} \cdot N_{pop} \cdot cos\left(\frac{\pi g}{2G_{max}}\right)\right\rfloor,$$
$$N_{\text{contrarian}} = \left\lfloor r_{\text{contrarian}} \cdot (N_{\text{pop}} - N_{\text{elite}})\right\rfloor. \tag{4.3}$$

In this formula, r_{elite} represents the proportion of elite antibodies, g denotes the current iteration number, G_{max} signifies the maximum number of iterations, and $r_{\text{contrarian}}$ indicates the proportion of reversed antibodies. The probability of breeding is calculated as follows:

$$p = a \cdot p_f(i) + (1 - a) \cdot p_d(i),$$
$$p_f(i) = \frac{fitness(i)}{\sum_{k=1}^{N_{clone}} fitness(k)},$$
$$p_d(i) = \frac{con(i)}{\sum_{k=1}^{N_{clone}} con(k)},$$
$$con(i) = \frac{N_{similar}}{N_{clone}}. \tag{4.4}$$

In this formula, a denotes the reproduction probability coefficient, N_{clone} signifies the number of remaining non-elite antibodies, and $N_{similar}$ indicates the number of other antibodies to be cloned that satisfy the similarity threshold (t_s). The similarity among antibodies to be cloned is comprehensively calculated using the following formula:

$$similarity(sol_1, sol_2) = 0.5 \cdot X_{sim} + 0.3 \cdot Y_{sim} + 0.2 \cdot Q_{sim}. \tag{4.5}$$

In this formula, X_{sim} denotes the similarity of maintenance measures, scored by the degree of measure matching, with the key units weighted double and averaged across all units. Y_{sim} represents resource allocation similarity, combining the time difference, work hour difference, and personnel matching, averaged over effective units. Q_{sim} indicates the quantum state similarity, calculated via the cosine similarity of complex vectors after validating the matrix. The probability of the suppression and elimination of reproduction are calculated as follows:

$$p' = \begin{cases} 0.5 \cdot p & con(i) > t_c \\ 0 & p < t_e \\ p & other \end{cases}. \tag{4.6}$$

In this formula, t_c and t_e represent the inhibition and elimination concentration thresholds for the probability of reproduction, respectively.

Step 5: Crossover mutation.

Initially, perform crossover operations on the cloned population by pairing adjacent antibodies. Denote the two antibodies as A and B, with a specified crossover probability. Select a crossover point K at random, corresponding to a row index that satisfies the condition $1 \leq K < U$. Subsequently, exchange the maintenance decisions and quantum states between row $K+1$ and the final row according to the following procedure:

$$X_1[k+1:,:] \leftrightarrow X_2[k+1:,:],$$
$$\alpha_1[k+1:,:] \leftrightarrow \alpha_2[k+1:,:]. \tag{4.7}$$

Finally, depending on the probability of mutation (P_m), a mutation operation is executed. The positions of the quantum bits within the maintenance measure's decision layer are randomly rearranged and then collapsed for decoding purposes. Simultaneously, the resource allocation matrix Y, corresponding to all inverted, cloned, and crossover-mutated antibodies, is reinitialized, marking the resources as unallocated. The rotation matrix for the mutation operation, based on the reference angle (θ), is as follows:

$$Rot_{matrix} = \begin{bmatrix} cos\theta & -sin\theta \\ sin\theta & cos\theta \end{bmatrix}. \tag{4.8}$$

Step 6: Present the currently optimal antibody.

All inverted, cloned, and crossover-mutated antibodies are first merged with those from the memory library, forming an intermediate population. After evaluation, identify and select the top N_{elite} antibodies demonstrating the highest fitness levels to update the memory library. Following this update, the optimal antibody from the current generation is then identified as the output.

Step 7: Evaluation of the termination criteria.

Should the maximum number of iterations be reached, the iterative process must be terminated and the results presented; if not, the process should continue with quadrant-based decision evolution applied to the population.

Step 8: Conducting an evolutionary population analysis within a four-quadrant decision-making framework.

Using the optimal elite antibody from the memory pool as a reference, the decision space is divided into four quadrants based on two dimensions: Consistency between the repair strategies of non-elite and elite antibodies, and the difference in their fitness. The quantum state's update rules are the following.

(1) If the strategies are consistent and non-elite fitness is superior, the quantum state remains unchanged.

(2) If the strategies are consistent but fitness is inferior, a small positive rotation encourages exploring better solutions along the original strategy.

(3) If the strategies are inconsistent but fitness is superior, a small negative rotation balances retaining the advantages and maintaining diversity.

(4) If the strategies are inconsistent and fitness is inferior, a larger positive rotation rapidly adjusts the strategy toward the elite antibody's effective approach.

$$\Delta\theta_{u,v} = \begin{cases} 0 & \text{if } v_c = v_e \text{ and } f_c \geq f_e \\ +\eta_s \cdot \theta_b & \text{if } v_c = v_e \text{ and } f_c < f_e \\ -\eta_e \cdot \theta_b & \text{if } v_c \neq v_e \text{ and } f_c \geq f_e \\ +\eta_d \cdot \theta_b & \text{if } v_c \neq v_e \text{ and } f_c < f_e \end{cases}. \tag{4.9}$$

In this formula, the variable θ_b denotes the reference rotation angle, η_s represents the reinforcement coefficient associated with the homogeneous strategy, η_e corresponds to the adjustment coefficient for advantage exploration, and η_d signifies the convergence coefficient related to the heterogeneous strategy. Figure 4 depicts the procedural framework of the AQIA.

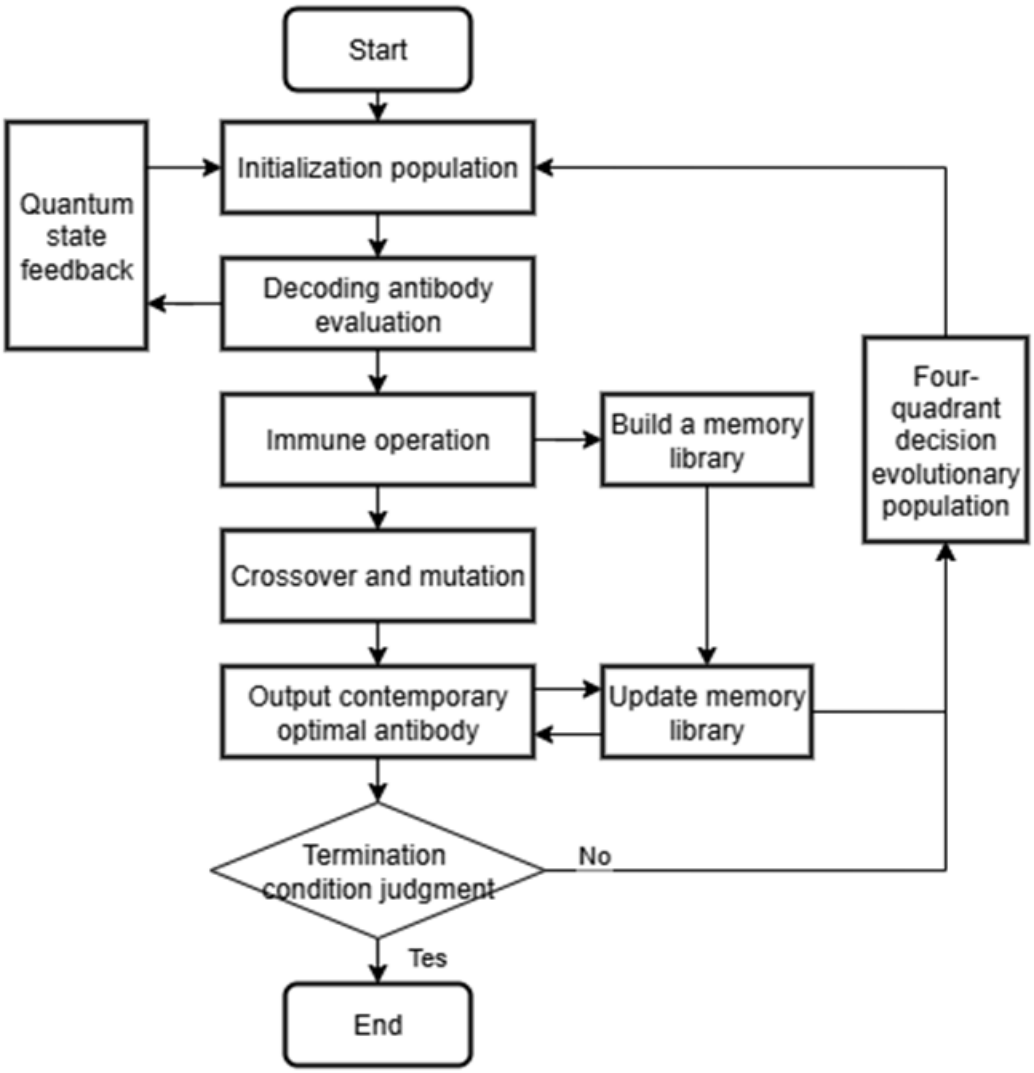

Figure 4. Diagrammatic representation of the AQIA.

5. Analysis of the case study

5.1. Description of the illustrative example

An aviation equipment maintenance facility must perform preventive maintenance on 12 operational units within a specified wartime readiness period. These units comprise three types (A, B, and C), with each type containing four units: One primary and three auxiliary. This maintenance ensures synchronized operation for an eight-hour task. The available maintenance personnel possess varying skill levels, graded from 1 to 4. Key constraints for this operation encompass the maximum allowable equivalent maintenance costs and the total equivalent working hours. Given these limitations, an optimal integrated maintenance plan is essential. To address this need for an optimal plan under the

aforementioned constraints, the specific configurations of the equipment categories and their associated mission requirements are detailed in Table 3.

Table 3. Equipment groups' parameters.

Types	α_m	β	K_m	U_m
A	1.2	0.018	3	4
B	1.1	0.015	2	4
C	1.1	0.012	2	4

Table 4 shows the initial state probability distributions and classifications of each combat unit.

Table 4. Parameters for each unit.

Unit	Category	State probability distribution of the unit				
		P(S1)	P(S2)	P(S3)	P(S4)	P(S5)
A1	Primary	0.05	0.10	0.15	0.30	0.40
A2	Auxiliary	0.10	0.15	0.25	0.30	0.20
A3	Auxiliary	0.15	0.20	0.25	0.25	0.15
A4	Auxiliary	0.10	0.15	0.20	0.35	0.20
B1	Primary	0.15	0.20	0.25	0.25	0.15
B2	Auxiliary	0.20	0.25	0.25	0.20	0.10
B3	Auxiliary	0.25	0.25	0.20	0.20	0.10
B4	Auxiliary	0.20	0.20	0.25	0.25	0.10
C1	Primary	0.25	0.25	0.20	0.20	0.10
C2	Auxiliary	0.30	0.25	0.20	0.15	0.10
C3	Auxiliary	0.35	0.25	0.15	0.15	0.10
C4	Auxiliary	0.30	0.20	0.20	0.20	0.10

Table 5 details the skill levels of the maintenance personnel and lists the benchmark equivalents for their respective working hours and costs. Here, the coefficients for work hour compression and cost escalation are set at 0.2 and 0.15, respectively.

Table 5. Reference parameters for maintenance personnel.

ID number	$s_{p1}(0.30)$	$s_{p2}(0.25)$	$s_{p3}(0.30)$	$s_{p4}(0.15)$	t_l	c_l	l_{pn}
P1	0.20	0.28	0.25	0.30	18	60	1
P2	0.55	0.60	0.48	0.58	16	80	2
P3	0.75	0.78	0.82	0.76	14	100	3
P4	0.92	0.95	0.93	0.90	12	120	4

The initial probability distribution across these states differs for each unit at the start of the maintenance interval. Additionally, it is assumed that the underlying state transition intensity matrix is uniform for all units and is defined as follows:

$$\Lambda_0 = \begin{bmatrix} 0 & 0 & 0 & 0 & 0 \\ 0.20 & -0.20 & 0 & 0 & 0 \\ 0 & 0.15 & -0.15 & 0 & 0 \\ 0 & 0 & 0.10 & -0.10 & 0 \\ 0 & 0 & 0 & 0.05 & -0.05 \end{bmatrix}.$$

Each unit may implement one of five selectable maintenance measures, each corresponding to specific maintenance effects that are aligned with the degree of degradation in the performance state and categorized accordingly.

$$A_{v_0} = \begin{bmatrix} 1 & 0 & 0 & 0 & 0 \\ 0 & 1 & 0 & 0 & 0 \\ 0 & 0 & 1 & 0 & 0 \\ 0 & 0 & 0 & 1 & 0 \\ 0 & 0 & 0 & 0 & 1 \end{bmatrix},$$

$$A_{v_1} = \begin{bmatrix} 0.10 & 0.25 & 0.35 & 0.20 & 0.10 \\ 0 & 0.20 & 0.40 & 0.30 & 0.10 \\ 0 & 0 & 0.30 & 0.45 & 0.25 \\ 0 & 0 & 0 & 0.60 & 0.40 \\ 0 & 0 & 0 & 0 & 1 \end{bmatrix},$$

$$A_{v_2} = \begin{bmatrix} 0.05 & 0.15 & 0.30 & 0.30 & 0.20 \\ 0 & 0.10 & 0.25 & 0.40 & 0.25 \\ 0 & 0 & 0.15 & 0.40 & 0.45 \\ 0 & 0 & 0 & 0.40 & 0.60 \\ 0 & 0 & 0 & 0 & 1 \end{bmatrix},$$

$$A_{v_3} = \begin{bmatrix} 0.02 & 0.08 & 0.20 & 0.40 & 0.30 \\ 0 & 0.05 & 0.15 & 0.35 & 0.45 \\ 0 & 0 & 0.10 & 0.30 & 0.60 \\ 0 & 0 & 0 & 0.20 & 0.80 \\ 0 & 0 & 0 & 0 & 1 \end{bmatrix},$$

$$A_{v_4} = \begin{bmatrix} 0 & 0 & 0 & 0 & 1 \\ 0 & 0 & 0 & 0 & 1 \\ 0 & 0 & 0 & 0 & 1 \\ 0 & 0 & 0 & 0 & 1 \\ 0 & 0 & 0 & 0 & 1 \end{bmatrix}.$$

5.2. Comparison and analysis of the algorithm's performance

To thoroughly assess the proposed algorithm's superiority, multidimensional comparative experiments were conducted under equal resource and parameter settings. The comparison included the traditional metaheuristics of the immune algorithm (IA), genetic algorithm (GA), and particle swarm optimization (PSO), the hybrid algorithms of the genetic particle swarm algorithm (GA-PSO) [25] and genetic tabu search algorithm (GA-TS) [26], and the unmodified quantum immune algorithm (QIA) as a control. This analysis focused on the dynamic convergence process (Figure 5) and static statistical indicators (Table 6), demonstrating its distinct advantages in solving complex constrained optimization problems.

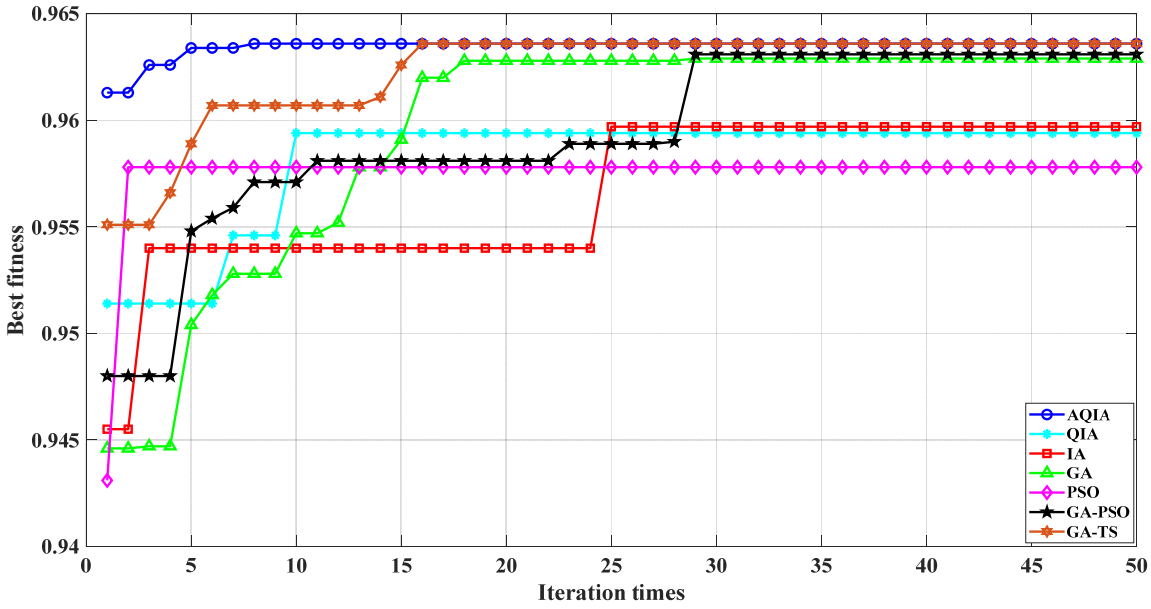

Figure 5. Comparative analysis of the algorithms' convergence.

As revealed in Figure 5, the AQIA demonstrates rapid convergence within the first 10 generations, a behavior indicative of a high-quality initial population that effectively circumvents unproductive search efforts. In contrast, traditional algorithms such as the IA and PSO exhibit slower convergence, stabilizing at inferior values—a clear reflection of their inefficient search strategies when handling complex constraints. The unmodified QIA performs moderately, highlighting the need for improvements. Although the GA shows some mid-phase search potential, it fluctuates and achieves lower accuracy than the AQIA. Although the hybrid algorithms GA-PSO and GA-TS achieve final convergence values comparable with those of the AQIA, their convergence paths are markedly slower and more erratic. This suggests that simple hybridization can improve the final solution's quality but cannot match the search efficiency gained from deeply integrated designs, underscoring the importance of maintaining the population's quality.

Table 6. Results of 20 independent algorithm runs.

Algorithm	Optimal value	Mean value	Standard deviation
AQIA	0.9636	0.9636	0
QIA	0.9594	0.9575	0.0020
IA	0.9597	0.9573	0.0027
GA	0.9626	0.9614	0.0016
PSO	0.9578	0.9529	0.0040
GA-PSO	0.9631	0.9622	0.0012
GA-TS	0.9636	0.9636	0

As shown in Table 6, both the AQIA and GA-TS achieved the highest optimal value (0.9636). However, GA-TS's convergence curve suggests this result requires a longer search time. Other algorithms, including the GA and GA-PSO, show nonzero standard deviations, indicating performance

fluctuations and limited reliability. PSO exhibits the poorest stability, consistent with its tendency toward premature convergence.

The experiment results indicate that the AQIA demonstrates high convergence speed, solution accuracy, and robustness in solving this joint optimization problem.

5.3. An empirical study of resource allocation methods

This study adopted a stepped "resource–personnel" comparative design to systematically examine the coupled effects of resource constraints and personnel configurations on maintenance efficiency. For the experimental group, resources were incrementally increased by 50%, starting from a minimum viable baseline, while maintaining a fixed personnel composition. Conversely, the control group tested various personnel allocations under a constant level of resource consumption. Each group underwent independent algorithmic iterations to determine the total task completion value. Critical resource transformation thresholds were identified on the basis of the marginal benefit peaks and troughs, with a trough defined as 10% below the peak. The detailed parameters governing this experimental framework are provided in Table 7.

Table 7. Experimental parameters.

Team designation	p_1	p_2	p_3	p_4	Fundamental feasible solution	(T, C)
Basic group	l_1	l_2	l_3	l_4	$(l_1,\ l_2,\ l_3)$	(207, 18)
Beginner group	l_2	l_2	l_3	l_4	$(l_2,\ l_2,\ l_3)$	(216, 14.4)
Intermediate group	l_2	l_3	l_3	l_4	$(l_2,\ l_3,\ l_3)$	(225, 14.4)
Advanced group	l_2	l_3	l_4	l_4	$(l_2,\ l_3,\ l_4)$	(234, 14.4)

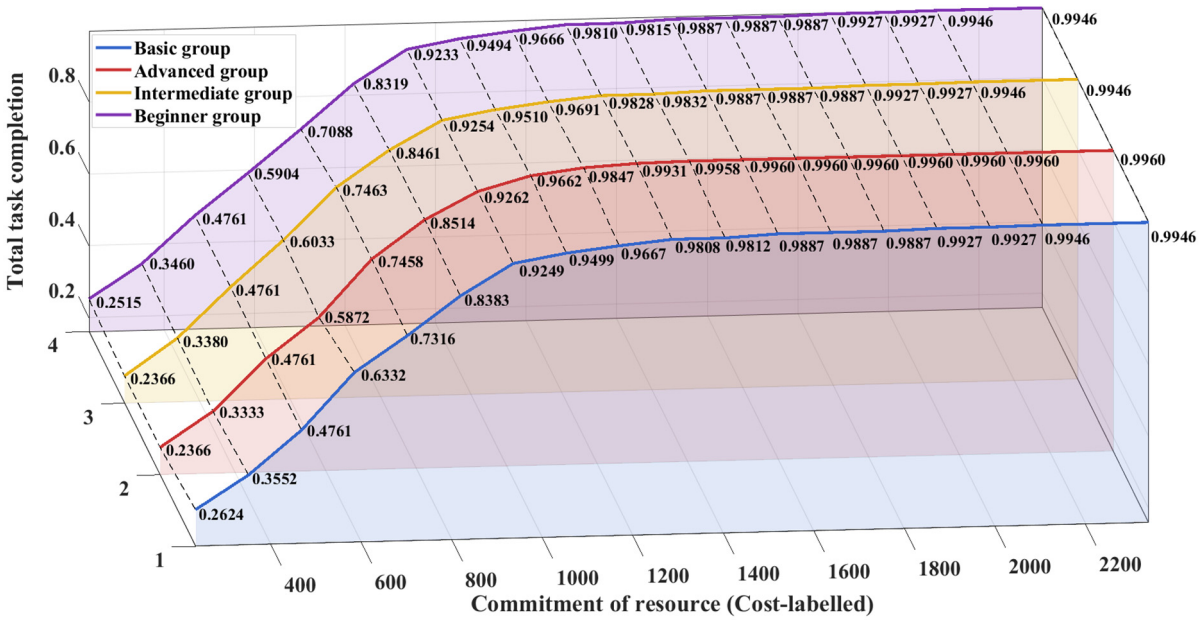

Figure 6. Experimental results (Part 1).

Figure 6 shows a clear three-phase pattern in resource distribution. In the contraction phase ($C \leq 643.5, h \leq 30.5$), the basic group reaches a local Pareto optimum in efficiency. During the growth

phase ($643.5 < C \leq 1053, h \leq 53$), the intermediate group improves efficiency by 4.3%. Later in this phase, the advanced group's breakthrough capacity creates a bimodal synergy, narrowing the efficiency gap with the intermediate group to 0.5%. In the abundant resource phase ($1053 < C \leq 1345.5$), the advanced group takes a leading role, driving task completion rates to their theoretical maximum under a resource surplus. This underscores the crucial role of elite human resources in achieving technological gains.

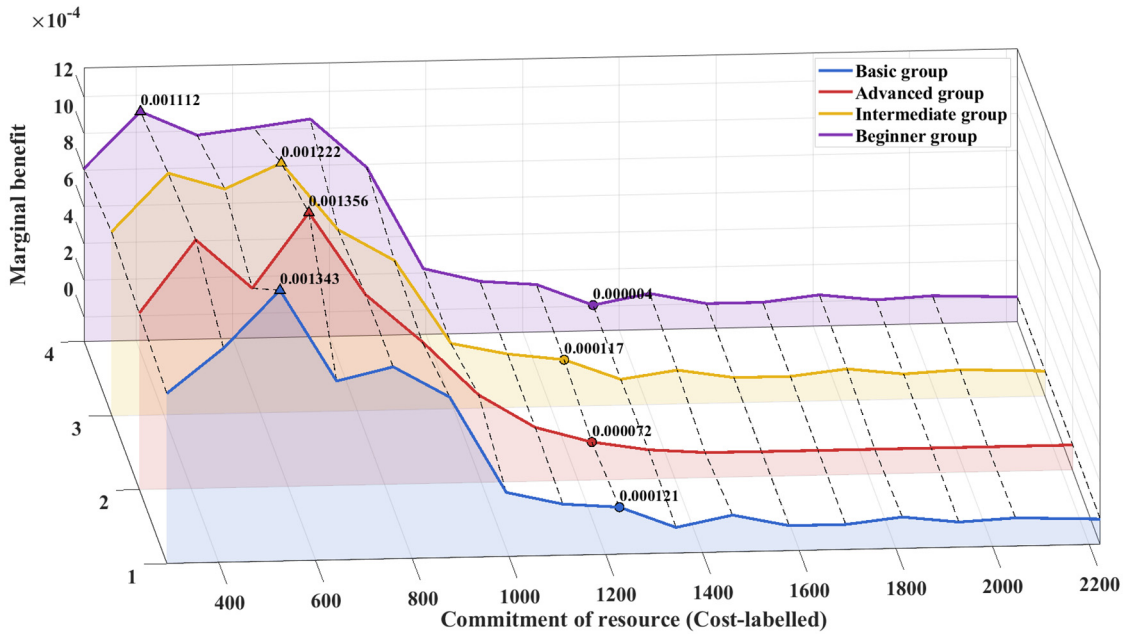

Figure 7. Experimental results (Part 2).

The marginal benefit curve presented in Figure 7 demonstrates a complex pattern of resource transformation. Notably, the beginner group reaches its maximum marginal benefit at an earlier point (C = 409.5); however, the magnitude of this peak is the lowest among all groups, being 24.3% less than that of the advanced group. This difference reflects an inherent limitation in the benefit ceiling for the beginner group. Moreover, the paradox observed in the advanced group's tightening zone, namely high marginal benefit coupled with low task completion, stems from the high resource intensity required to activate top-tier personnel, a prerequisite for unlocking their breakthrough potential.

The benefit trough points (solid markers) serve as critical early warning indicators. For instance, trough values approaching zero for the beginner group signal that resource input has entered a failure zone. Conversely, the marginal benefit of the advanced group after Point A declines to zero, reaching the theoretical efficiency frontier. This contrast reveals that the marginal benefit delineates the upper limit of potential inherent in a personnel structure, whereas realizing this potential is contingent upon matching resource conditions. Consequently, the marginal benefit curve should inform resource allocation decisions as a supplementary tool, not stand as an independent efficiency metric. In conclusion, the beginner group should be discontinued.

To comprehensively investigate the universal principles underlying maintenance strategies, the limited resources of the advanced group at both the peak and trough efficiency points were used to perform algorithmic optimization for the remaining groups. As a result, the optimal allocation of maintenance strategies across six distinct fixed resource scenarios was established, as shown in Table 8.

Table 8. Allocation of optimal maintenance strategies under resource constraints.

Unit	Benefit peak points			Benefit trough points		
	Basic group	Intermediate group	Advanced group	Basic group	Intermediate group	Advanced group
A1	(v_1, p_1)	(v_1, p_1)	(v_1, p_1)	(v_3, p_3)	(v_3, p_2)	(v_4, p_3)
A2	(v_1, p_2)	(v_1, p_3)	(v_1, p_4)	(v_4, p_4)	(v_4, p_4)	(v_4, p_3)
A3	(v_4, p_4)	(v_4, p_4)	(v_4, p_3)	(v_4, p_4)	(v_4, p_4)	(v_4, p_3)
A4	v_0	v_0	v_0	(v_4, p_4)	(v_4, p_4)	(v_4, p_3)
B1	(v_1, p_2)	(v_1, p_1)	(v_1, p_1)	(v_3, p_3)	(v_2, p_1)	(v_1, p_1)
B2	v_0	v_0	v_0	(v_3, p_3)	(v_3, p_2)	(v_4, p_3)
B3	(v_3, p_3)	(v_2, p_2)	(v_1, p_2)	$(v_3,\ p_3)$	(v_3, p_2)	v_0
B4	v_0	v_0	v_0	(v_2, p_2)	(v_2, p_1)	(v_4, p_4)
C1	(v_3, p_3)	(v_2, p_2)	(v_3, p_2)	(v_1, p_1)	(v_1, p_1)	(v_1, p_1)
C2	v_0	v_0	v_0	(v_4, p_4)	(v_4, p_4)	(v_4, p_4)
C3	(v_4, p_4)	(v_4, p_4)	(v_4, p_3)	(v_4, p_4)	(v_4, p_4)	(v_4, p_4)
C4	v_0	v_0	v_0	(v_2, p_2)	(v_2, p_2)	(v_4, p_4)
D_{total}	0.6681	0.6530	0.6462	0.9801	0.9772	0.9902

Table 8 illustrates that under conditions of resource constraints, personnel skill misalignments hinder strategic resilience. Specifically, the advanced group faces a skills gap resulting from the direct transition from l_2 to l_3, which impairs their ability to sustain equivalent skill levels during the maintenance of Unit A1. This leads to a 15% cost increase compared with the baseline group's plan. Simultaneously, the maintenance activities for Unit B3 are forced to be downgraded, triggering a negative feedback loop; a similar situation is observed in the intermediate group. In contrast, the basic group, benefiting from a stable alignment of personnel skills, demonstrates strong adaptability by adopting a low-level maintenance strategy v_1 for Unit A1. This strategy enables the reallocation of greater maintenance resources to Unit B3, thereby enhancing the task completion outcomes.

Under conditions of abundant resources, the deployment density of senior personnel dictates the ceiling for a maintenance strategy's potential effectiveness. The senior team, using a dual top-tier personnel configuration, is uniquely positioned within Unit A1 to implement an advanced maintenance strategy. In contrast, the baseline team, constrained to a single top-tier personnel structure, can only adopt a secondary combination of maintenance measures as its optimal approach. This discrepancy is especially pronounced at the point of minimal efficiency: The advanced cohort simultaneously applies multiple v_4 maintenance procedures, resulting in a higher task completion rate. Although the intermediate cohort has similar resources, their efforts are directed toward lower-priority tasks, which constrains their capacity. For instance, Unit C1 relies on l_2 to perform v_1, thereby impeding the replication of an equivalent degree of focused effort.

5.4. Policy optimization from the perspective of continuous tasks

Previous research has indicated that the four-person maintenance strategy is significantly constrained by resource availability. Within the existing human resource framework, this strategy remains feasible for supporting single-cycle static maintenance and small-scale operational demands. However, in actual combat conditions, equipment units are generally required to undertake continuous multicycle operational tasks, which involve considerable fluctuations in the resource levels. To address

these challenges, a dynamic five-person configuration, designated as $(l_1,\ l_2,\ l_3,\ l_4,\ l_4)$ is proposed. Specifically, this approach involves implementing a hibernation mechanism in which one Grade l_4 employee is placed into hibernation during periods of resource scarcity, whereas one Grade l_1 employee is placed into hibernation during times of resource abundance, concurrently reinstating the dual Grade l_4 framework. The model simulates continuous operations within a multicycle maintenance context analogous to real combat scenarios, with the detailed parameters provided in Table 9 below.

Table 9. Criteria for sustained combat operations.

Task number	1	2	3	4	5	6
Duration	8	12	10	5	6	14
Maintenance resources	(585, 33)	(1170, 58)	(1521, 73)	(351, 23)	(468, 28)	(1521, 73)

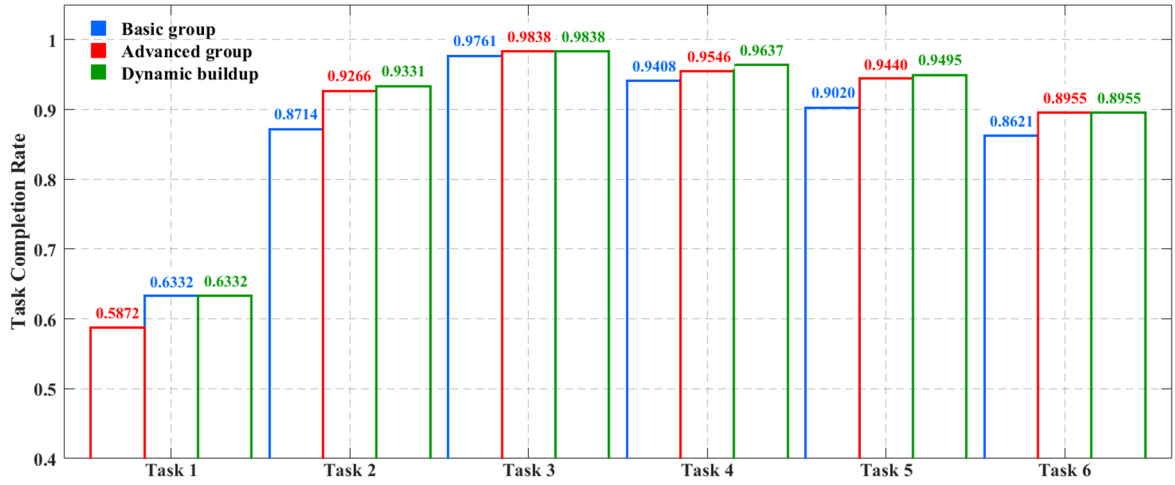

Figure 8. Experimental results (Part 3).

As shown in Figure 8, the dynamic five-person team configuration secures the top rank in every mission phase, demonstrating consistent superiority over static configurations in a multicycle operational context. The overall mission completion rate for this configuration across multiple cycles is 0.8955, representing an absolute improvement of 3.35% compared with the static group with the lowest performance (the basic group at 0.8621). This performance advantage is attributed to the dynamic sleep mechanism's proactive adjustment to resource variability, enabling the system to maintain a near-optimal operational state throughout the entire cycle.

Table 10. Number of advanced maintenance measures.

Task number		1	2	3	4	5	6
Basic group	v_3	2	4	5	1	0	5
	v_4	2	4	6	1	1	6
Advanced group	v_3	0	2	0	0	0	0
	v_4	3	8	12	1	2	12
Dynamic buildup	v_3	2	2	0	1	0	0
	v_4	2	8	12	1	2	12

Table 10 reveals that the core superiority of the dynamic maintenance strategy is rooted in the synergy between two mechanisms: Adaptive resource elasticity and cumulative state effects. During intervals marked by resource constraints (Tasks 1 and 4), the dynamic group closely mirrors the conservative approach utilized by the baseline group, thereby establishing an initial reliability advantage. In contrast, in periods characterized by resource abundance and surplus (Tasks 2 and 6), the dynamic group's allocation to advanced maintenance measures matches or surpasses that of the advanced group. This adaptive member switching creates a pronounced state inheritance effect, culminating in the enhanced coverage efficiency that characterizes the overall maintenance strategy.

Empirical studies show that the dynamic architecture offers new methods to enhance the sustained operational effectiveness of equipment formations. This framework applies to standard multiphase combat scenarios, including support for carrier-based aircraft groups.

6. Conclusions

This study focuses on equipment groups, examining selective maintenance decisions and personnel allocation under resource constraints. An environmental coefficient is introduced to capture the impact of varying subtask environments on the units' degradation. A nonhomogeneous Markov model is used to calculate the probability of task completion following a unit's degradation; these unit-level probabilities then determine the completion probabilities for their respective subtasks. A maintenance optimization model is developed to maximize the overall single-cycle task completion probability and is solved using an AQIA. Case studies are conducted for experimental analysis and optimization. Key findings include the following.

(1) The integrated optimization scheduling model based on the AQIA outperforms traditional algorithmic search models, showing superior convergence speed and solution quality compared with other hybrid metaheuristic algorithms.

(2) A maintenance personnel structure designed for limited resources can achieve Pareto optimality in local efficiency from a single-cycle maintenance perspective.

(3) A dynamic personnel allocation structure effectively mitigates resource fluctuations and achieves optimal efficiency locally and globally, making it the preferred strategy in multitask battlefield scenarios.

(4) The model developed in this research provides theoretical guidance and technical support for maintenance decisions regarding equipment groups in both static maintenance and dynamic combat, offering valuable insights to improve the probability of task completion in coordinated multiequipment operations.

Author contributions

Yang Jiao: Conceptualization, methodology, software, formal analysis, investigation, writing—original draft.

Qiu-Xiang Tao*: Supervision, validation, project administration, writing—review and editing, funding acquisition.

Hui Liu, Qi-Rui Peng, and Zhi-Cheng Zhou: Data curation, experimental investigation, visualization, with contributions listed in descending order of appearance.

Use of Generative AI tools

No artificial intelligence (AI) tools were used in the creation of this article.

Acknowledgments

The author sincerely thanks the editor and reviewers for their constructive comments and suggestions.

This work is supported by the National Natural Science Foundation of China (Grant No. 72261027) and the University-Level Graduate Innovation Special Fund Supported Project of Nanchang Hangkong University (YC2025-077).

Conflict of interest

The authors declare that they have no conflicts of interest.

References

1. S. B. Yin, L. Zhou, M. Zhao, Z. H. Ren, Research on replacement and maintenance decision of degraded equipment based on maintenance effectiveness, *Mil. Oper. Res. Assess.*, **35** (2021), 36–42. https://doi.org/10.19949/j.ams.mora.20210330.01
2. N. Gupta, I. Ali, A. Bari, Fuzzy goal programming approach in selective maintenance reliability model, *Pak. J. Stat. Oper. Res.*, **9** (2013), 321–331. https://doi.org/10.18187/pjsor.v9i3.654
3. I. Ali, S. S. Hasan, Bi-criteria optimization technique in stochastic system maintenance allocation problem, *Am. J. Oper. Res.*, **3** (2013), 17–29. https://dx.doi.org/10.4236/ajor.2013.31002
4. J. F. Wang, G. W. Jia, J. C. Lin, Z. Hou, Cooperative task allocation for heterogeneous multi-UAV using multi-objective optimization algorithm, *J. Cent. South Univ.*, **27** (2020), 432–448. https://doi.org/10.1007/s11771-020-4307-0
5. Z. Y. Jia, J. Q. Yu, X. L. Ai, X. Xu, D. Yang, Cooperative multiple task assignment problem with stochastic velocities and time windows for heterogeneous unmanned aerial vehicles using a genetic algorithm, *Aerosp. Sci. Technol.*, **76** (2018), 112–125. https://doi.org/10.1016/j.ast.2018.01.025
6. A. Khatab, C. Diallo, U. Venkatadri, Z. Liu, E. H. Aghezzaf, Optimization of the joint selective maintenance and repairperson assignment problem under imperfect maintenance, *Comput. Ind. Eng.*, **125** (2018), 413–422. https://doi.org/10.1016/j.cie.2018.09.012
7. E. H. Aghezzaf, C. Diallo, A. Khatab, U. Venkatadri, A joint selective maintenance and multiple repairperson assignment problem, *Proc. 7th Int. Conf. Ind. Eng. & Syst. Manag.*, (2017), 317–322.
8. X. Y. Wang, Y. Tian, X. M. Qiang, J. Qian, Mission assignment model for anti-missile combat based on cooperative efficiency, *J. Air Force Eng. Univ.*, **14** (2013), 27–31. https://doi.org/10.3969/j.issn.1009-3516.2013.04.007
9. X. N. Zhu, X. P. Zhu, R. Yan, R. Peng, Optimal routing, aborting and hitting strategies of UAVs executing hitting the targets considering the defense range of targets, *Rel. Eng Syst. Safety*, **215** (2021), 107811. https://doi.org/10.1016/j.ress.2021.107811

10. C. Diallo, U. Venkatadri, A. Khatab, Z. Liu, E. H. Aghezzaf, Optimal joint selective imperfect maintenance and multiple repairpersons assignment strategy for complex multicomponent systems, *Int. J. Prod. Res.*, **57** (2019), 4098–4117. https://doi.org/10.1080/00207543.2018.1505060
11. T. Jiang, Y. Liu, Selective maintenance strategy for systems executing multiple consecutive missions with uncertainty, *Rel. Eng. & Syst. Safety*, **193** (2020), 106632. https://doi.org/10.1016/j.ress.2019.106632
12. Z. Y. Zhen, P. Zhu, Y. X. Xue, Y. X. Ji, Distributed intelligent self-organized mission planning of multi-UAV for dynamic targets cooperative search-attack, *Chin. J. Aeronaut.*, **32** (2019), 2706–2716. https://doi.org/10.1016/j.cja.2019.05.012
13. M. H. Wang, Z. C. Zhou, R. Zhang, G. S. Chen, Firepower distribution model of amphibious attack ship for air self-defense combat, *Fire Contr. Command Contr.*, **45** (2020), 127–131. https://doi.org/10.3969/j.issn.1002-0640.2020.12.024
14. W. N. Ma, Q. W. Hu, J. Chen, X. S. Jia, Joint optimization of selective maintenance decision-making and task allocation for equipment groups, *Acta Armamentarii*, **45** (2024), 407–416. https://doi.org/10.12382/bgxb.2022.0649
15. A. Amjadian, R. O'Neil, A. Khatab, J. Chen, U. Venkatadri, C. Diallo, Optimising resource-constrained fleet selective maintenance with asynchronous maintenance breaks, *Int. J. Prod. Res.*, **63** (2025), 2385–2407. https://doi.org/10.1080/00207543.2024.2403114
16. Y. P. Zhang, Z. J. Su, L. Shi, M. Y. Zhang, Optimization method for maintenance decision of complex systems based on nested particle swarm optimization. *Comput. Integr. Manuf. Syst.*, **29** (2023), 3800–3811. https://doi.org/10.13196/j.cims.2021.0399
17. K. Chaabane, A. Khatab, C. Diallo, E. H. Aghezzaf, U. Venkatadri, Integrated imperfect multimission selective maintenance and repairpersons assignment problem, *Rel. Eng. Syst. Safety*, **199** (2020), 106895. https://doi.org/10.1016/j.ress.2020.106895
18. K. Moghaddam, J. Usher, A new multi-objective optimization model for preventive maintenance and replacement scheduling of multi-component systems, *Eng. Optim.*, **43** (2011), 701–719. https://doi.org/10.1080/0305215X.2010.512084
19. R. O'Neil, A. Khatab, C. Diallo, A. Saif, Joint selective maintenance and mission abort decisions for mission-critical systems, *Rel. Eng. Syst. Safety*, **264** (2025), 111358. https://doi.org/10.1016/j.ress.2025.111358
20. Y. Liu, Reliability modelling and maintenance decision-making for multi-state complex systems, Univ. Electron. Sci. Technol. China, (2010). https://doi.org/10.7666/d.Y1851647
21. L. Cao, Z. T. Wang, L. Chen, H. S. Li, S. Gao, Z. L. Zhang, Neural network ensemble based on improved quantum immune algorithm, *Comput. Eng. Appl.*, **56** (2020), 142–147. https://doi.org/10.3778/j.issn.1002-8331.2005-0357
22. Y. Y. Li, L. C. Jiao, Quantum immune clone multi-objective optimization algorithm, *J. Electron. Inf. Technol.*, **6** (2008), 1367–1371. https://doi.org/10.3724/SP.J.1146.2006.01709
23. Y. Jing, Y. K. Liu, M. K. Bi, Quantum-inspired immune clonal algorithm for railway empty cars optimization based on revenue management and time efficiency, *Cluster Comput.*, **22** (2019), 545–554. https://doi.org/10.1007/s10586-017-1292-7
24. X. H. Liu, M. Y. Shan, R. L. Zhang, L. H. Zhang, Green vehicle routing optimization based on carbon emission and multi-objective hybrid quantum immune algorithm, *Math. Probl. Eng.*, **4** (2018), 1–9. https://doi.org/10.1155/2018/8961505

25. T. Zhang, Y. S. Liu, Integrated task priority scheduling using genetic particle swarm algorithm, *Radar ECM*, **45** (2025), 1–6. https://doi.org/10.19341/j.cnki.1009-0401.2025.03.001
26. D. Ni, Research on a hybrid metaheuristic scheduling algorithm for multi-station robot handling of lithium batteries, *Electron. Meas. Technol.*, **48** (2025), 128–135. https://doi.org/10.19651/j.cnki.emt.2518027

AIMS Press